

Effects of in-chain and off-chain substitutions on spin fluctuations in the spin-Peierls compound CuGeO_3

P. Lemmens, M. Fischer, and G. Güntherodt

2. Physikalisches Institut, RWTH-Aachen, 52056 Aachen, Germany

C. Gros

Institut für Physik, Universität Dortmund, 44221 Dortmund, Germany

P. G. J. van Dongen

Theoretische Physik III, Universität Augsburg, 86135 Augsburg, Germany

M. Weiden, W. Richter, C. Geibel, and F. Steglich

FB Technische Physik, TH-Darmstadt, 64289 Darmstadt, Germany

(Received 30 December 1996)

The effect of in-chain and off-chain substitutions on one-dimensional (1D) spin fluctuations in the spin-Peierls compound CuGeO_3 has been studied using Raman scattering in order to understand the interplay between defect induced states, enhanced spin-spin correlations, and the ground state of low-dimensional systems. In-chain and off-chain substitutions quench the spin-Peierls state and induce 3D antiferromagnetic order at $T \leq 5$ K. Consequently the suppression of a 1D gap-induced mode as well as a constant intensity of a spinon continuum are observed at low temperatures. A 3D two-magnon density of states now gradually extends to higher temperatures $T \leq 60$ K compared with pure CuGeO_3 . This effect is more pronounced in the case of off-chain substitutions (Si) for which a Néel state occurs over a larger substitution range, starting at very low concentrations. Besides, additional low energy excitations are induced. These effects, i.e., the shift of a dimensional crossover to higher temperatures are due to an enhancement of the spin-spin correlations induced by a small amount of substitutions. The results are compared with recent Monte Carlo studies on substituted spin ladders, pointing to a similar instability of coupled, dimerized spin chains and spin ladders upon substitution. [S0163-1829(97)03621-7]

I. INTRODUCTION

Quantum effects in low-dimensional antiferromagnetic spin systems have attracted an intensive theoretical and experimental interest in recent years. One of these effects is the formation of a continuum of spin fluctuations in one-dimensional (1D) spin-1/2 chains.¹ The magnetic excitations of the uniform $s=1/2$ Heisenberg antiferromagnetic chain are indeed dominated by strong fluctuations derived using the Bethe ansatz. They consist of delocalized or unbound solitonlike spinon excitations prohibiting a magnetically ordered state. The spinon continuum is enclosed by an upper and lower dispersion relation of the form $E_q^2 = \pi J |\sin(q_c/2)|$ and $E_q^1 = (\pi/2)J |\sin(q_c)|$, respectively.^{1,2} The existence of this continuum was verified in neutron experiments on the compound KCuF_3 (Ref. 3) and later in CuGeO_3 .⁴ Of particular importance in this sense is the spin-Peierls (SP) transition leading to a singlet ground state of the formed dimers and the opening of a spin gap near the lower boundary of the continuum. The modification of the excitation scheme in the dimerized state is theoretically not completely settled. The change under dimerization from spinons with $s=1/2$ to excitations with $s=1$ should lead to a redistribution of density of states from the spinon continuum into its lower dispersing limit. This may be understood as a localizing, pair-binding effect of the excitation gap⁵ that leads

to enhanced spinon-spinon interaction. The spin-spin correlation length changes from an algebraic to an exponential decay.

The compound CuGeO_3 initially appeared as an ideal spin-Peierls compound with a high $T_{\text{SP}}=14$ K and a stable lattice which allows for several types of substitutions.⁶⁻⁹ Later, however, evidence appeared that its behavior is complicated due to competing exchange interactions.^{10,11} The strong frustration of the spin system may drive or at least stabilize the dimerization transition in this compound. CuGeO_3 consists of chains of spin-1/2 Cu^{2+} ions along the c axis coupled by antiferromagnetic 98° superexchange through oxygen orbitals.^{6,7,12} This special superexchange geometry causes a strong sensitivity of the exchange on changes of the Cu-O-Cu bond angle. A bond angle close to the critical 90° leads to a comparatively small antiferromagnetic nearest-neighbor (NN) exchange, J_{c1} , and a frustrated next-nearest-neighbor (NNN) exchange, J_{c2} , that strongly depends on the local surrounding of the oxygen.¹³

The exchange along the Cu-O-Cu chains can be modeled by a 1D Hamiltonian including the competing NN and NNN interactions ($\sim \alpha$) and the dimerization δ .¹⁰

$$H = J_{c1} \sum_i \{ [1 + \delta(-1)^i] \mathbf{S}_i \cdot \mathbf{S}_{i+1} + \alpha \mathbf{S}_i \cdot \mathbf{S}_{i+2} \}. \quad (1)$$

Using neutron scattering results⁷ the following exchange constants were derived: $J_{c1}=150$ K, $J_{c2}\approx 36$ K, with the frustration parameter $\alpha=J_{c2}/J_{c1}=0.24-0.36$ close to or larger than a critical $\alpha_{cr}=0.2411$.¹⁰ For increasing $\alpha\geq\alpha_{cr}$ an exponentially small excitation gap exists which evolves to $\Delta=J_{c1}/4$ in a valence bond solid with $\alpha=0.5$.¹⁴ For CuGeO_3 a singlet-triplet gap $\Delta_{SP}=24-30$ K (Refs. 7 and 15) and a successive gap of similar size, separating the singlet-triplet excitation from a continuum of unbound spinons, were found in neutron scattering below T_{SP} .¹⁶ Additionally, well-behaved quasimagnon branches were observed below T_{SP} (Ref. 7) that clearly mark the change of the magnetic response from the uniform to the dimerized state.

Due to the non-negligible interchain exchange with $J_b=0.1J_{c1}$,⁷ comparable to and competing with the frustrated NNN exchange, the compound develops 3D magnetic correlations below 15 K. This may also be the origin of the Néel ordering observed for $T\leq 5$ K in substituted samples if the coherent singlet ground state is locally destroyed. Independent of the type of substitution, T_N is always of the order of 5 K and well separated from the spin-Peierls temperature of weakly substituted samples. In an intermediate concentration range a coexistence of T_{SP} and T_N is observed.¹⁷⁻¹⁹

Raman experiments on CuGeO_3 proved to be a versatile tool to investigate magnetic excitations due to their high resolution and large scattering cross section. Spin-Peierls active phonon modes together with a gap-induced mode at 30 cm^{-1} ($\approx 2\Delta_{SP}$) and a two-magnon density of states with a cutoff at 226 cm^{-1} were detected for $T<T_{SP}$.⁸ More interesting is the broad continuum from 100 to 500 cm^{-1} observed for $T>T_{SP}$ and the strong redistribution of its intensity into the two-magnon signal observed in the dimerized state.²⁰⁻²²

As shown recently, the continuum and the gap-induced mode are described by frustration-induced Heisenberg exchange scattering.²³ In these calculations a dimerization of the exchange constants of the Heisenberg and the Raman operator is taken into account as described by Eqs. (1) and (2). The Raman operator in A_{1g} symmetry with the dimerization γ and the frustration β is proportional to²⁴

$$H_R \propto \sum_i \{ [1 + \gamma(-1)^i] \mathbf{S}_i \cdot \mathbf{S}_{i+1} + \beta \mathbf{S}_i \cdot \mathbf{S}_{i+2} \}. \quad (2)$$

A very important point to note is that in the uniform state ($\delta=\gamma=0$), Raman intensity in the temperature range for negligible interchain coupling ($J_b \sim 15\text{ K} \ll T < J \sim 150\text{ K}$), is induced by the NNN term in Eqs. (1) and (2). When $\beta-\alpha=0$, the Raman Hamiltonian commutes with the Heisenberg Hamiltonian and there is no Raman scattering.²³ For lower temperatures these constraints are relaxed due to the interchain coupling. In this way the observed scattering continuum (above and below T_{SP}) and the gap-induced mode at 30 cm^{-1} (below T_{SP}) can be modeled by 1D spinon excitations. The parameters used are the exchange coupling constant $J_{c1}=150$ K and the frustration $|\beta-\alpha|=0.24$ derived from neutron scattering and susceptibility measurements.¹⁰ All other scattering contributions are negligible within a 1D model.²³

However, the evolution to the quasi-3D two-magnon density of states for $T<T_{SP}$ and the related quasimagnon disper-

TABLE I. Investigated single crystals $(\text{Cu}_{1-x}\text{Zn}_x)(\text{Ge}_{1-y}\text{Si}_y)\text{O}_3$ with their T_{SP} and T_N determined by SQUID magnetometry. T_{cross} is derived by Raman scattering and marks a crossover from 3D to 1D behavior in the spin excitations. A dash (–) denotes no observation of a phase transition.

x (Zn)	y (Si)	T_{SP}/K	T_N/K	T_{cross}/K
0	0	14.3	–	11
0.018		12.8	–	11
0.035		11	2.5	11
0.06		–	4	23
	0.022	–	5	25
	0.04	–	4.5	30
	0.06	–	2.5	35
	0.1	–	–	50

sions emerging out of the spinon continuum as observed in neutron scattering remain to be explained. This dimensional crossover from 1D to 3D upon cooling and the observation of a 3D magnetically ordered state in substituted samples at lower temperatures ($T\leq 5$ K) are pointing to an interplay of the spin-Peierls order parameter with 3D magnetic interactions that should be further clarified. This motivated our Raman study on in- and off-chain substituted single crystals of CuGeO_3 .

The paper is organized as follows. In Sec. II we describe the experimental setup and the samples investigated. In Sec. III we present results of magnetic Raman scattering with its discussion in Sec. IV. Section V contains a summary of our results.

II. EXPERIMENT

We have performed Raman scattering experiments on well-characterized single crystals in quasibackscattering geometry with the polarization of incident and scattered light parallel to Cu-O chains (c axis). In other scattering geometries no magnetic scattering contribution was observed. The experiments were performed with the $\lambda=514.5\text{-nm}$ excitation line of an Ar laser and a laser power below 0.2 W/cm^2 . The incident radiation does not increase the temperature of the sample by more than 1 K. The samples themselves are glued onto a copper sample holder and immersed in flowing He-exchange gas.

Here we present results on single crystals of $(\text{Cu}_{1-x}\text{Zn}_x)\text{GeO}_3$ and $\text{Cu}(\text{Ge}_{1-y}\text{Si}_y)\text{O}_3$ with $0\leq x\leq 0.06$ and $0\leq y\leq 0.1$ (see Table I). In previous studies the solubility range and phase homogeneity were checked for $0\leq x\leq 0.1$ and $0\leq y\leq 0.5$ and confirmed by using SQUID-magnetometry, x-ray scattering and thermal expansion measurements on both poly- and single crystals.^{25,26} In the case of Si substitution a disagreement is found between poly- and single crystals concerning the phase boundaries of T_{SP} vs y .²⁷ This is due to a growth of single crystals close to the decomposition temperature of the compound which shifts to lower temperature in Si-substituted samples. As a result oxygen nonstoichiometry and disorder are expected.^{27,28} This is confirmed by phonon Raman scattering. In Si-substituted single crystals several symmetry forbidden modes of pure CuGeO_3 are observed due to the relaxed momentum conser-

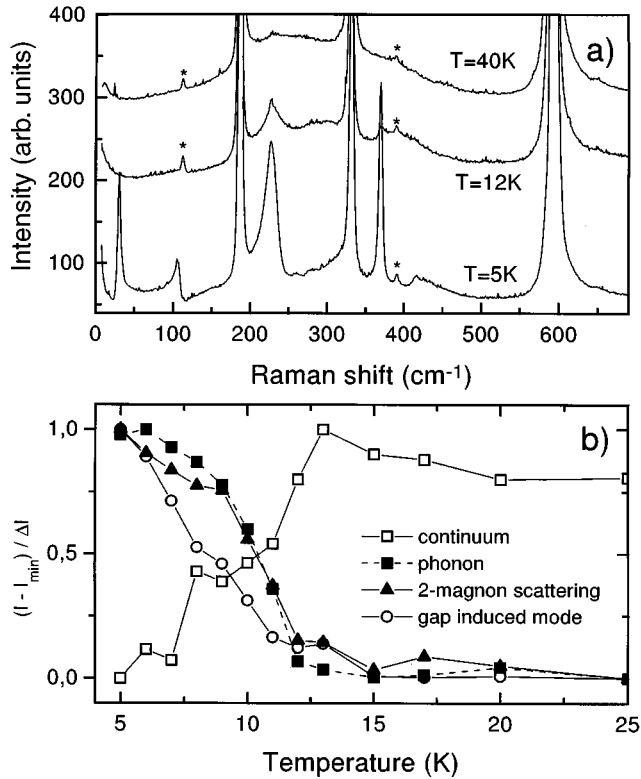


FIG. 1. Raman scattering intensity of CuGeO₃ (a) for temperatures between 5 and 40 K and (b) temperature dependence of the renormalized intensity of the spinon continuum, the Peierls-transition-induced phonon at 370 cm⁻¹, the two-magnon density of states cutoff at 226 cm⁻¹, and the gap-induced mode at 30 cm⁻¹. Additional symmetry forbidden modes due to a slight misalignment of the sample are marked by an asterisk.

vation. In addition static and temperature dependent defect modes are observed. For a complete description we refer to a forthcoming publication.²⁹

III. RESULTS

In the case of magnetic Raman scattering experiments in CuGeO₃ the results may be divided into three temperature regimes, as first described by van Loosdrecht *et al.*²⁰ At high temperatures a broad, quasielastic tail is visible. This tail is due to diffusive processes and follows roughly a $1/\omega$ dependence, with ω the Raman shift of the experiment. At lower temperature, $15\text{K} \leq T \leq 60\text{K}$ a broad continuum for $100\text{ cm}^{-1} \leq \omega \leq 500\text{ cm}^{-1}$ is observed which is assigned to the spinon continuum.^{20,23} Below $T_{\text{SP}} = 14\text{K}$ several new modes appear: three phonons at 105 cm⁻¹, 370 cm⁻¹, and 820 cm⁻¹ (with lower intensity), a two-magnon scattering cutoff at 226 cm⁻¹ and a gap-induced mode at 30 cm⁻¹. We will concentrate here on the temperature range $T \leq 60\text{K}$ and the effect of substitutions on the spinon continuum and the Peierls-transition-induced modes at 30, 226, and 370 cm⁻¹. As an example we show Raman spectra of pure CuGeO₃ in Fig. 1(a) for temperatures between 5 and 40 K.

While the occurrence of the spin-Peierls induced Raman modes is well established, their intensity was not studied in detail.^{8,20} However, the intensity as function of temperature

and substitution gives important information about the evolution of the singlet-triplet excitations as shown in Fig. 1(b) for pure CuGeO₃. While the intensity of the spinon continuum was determined by integrating the intensity between 100 and 500 cm⁻¹, subtracting a linear background and the phonons, the intensity of the two-magnon density of states was determined at the frequency of 226 cm⁻¹. At T_{SP} the scattering intensity of the spinon continuum clearly shows a maximum as function of temperature. The following sharp decrease toward low temperatures is counteracted by the increase of the intensities at 226 and 370 cm⁻¹. The gap-induced mode at 30 cm⁻¹ emerges at lower temperatures, i.e., below 11 K due to the evolution of a long range coherent, dimerized state below T_{SP} . The competition between the 1D spinon continuum, the quasi-3D two-magnon density of states and the Peierls-active phonon marks the proposed dimensional crossover of the compound at $T_{\text{cross}} = 11\text{K}$ induced by the spin-Peierls transition. T_{cross} is defined here as the temperature of half maximum intensity of the phonon. It should be noted that the behavior of the two-magnon signal at 226 cm⁻¹ is completely different from conventional magnetic light scattering in 3D antiferromagnets (AF) close to T_N or paramagnon scattering above T_N .³⁰ In 3D AF the two-magnon scattering shows a strong broadening of the line shape and shifts to lower frequencies with increasing temperature. Additionally, the integrated intensity shows a large increase at T_N and is therefore observable up to high temperatures. In CuGeO₃ we see close to T_{SP} neither a shift of the two-magnon signal to lower frequency nor a broadening. The intensity of both the two-magnon signal and the phonon at 370 cm⁻¹ emerge at $T \leq T_{\text{SP}}$ without a preceding energy renormalization. This aspect is confirmed by neutron scattering in the sense that magnons with a well-defined dispersion relation exist^{7,16} only for $T \leq T_{\text{SP}}$. Questions arise concerning the character and dimensionality of the underlying excitations. This problem will be addressed after discussing the results on substituted samples.

The onset of the 1D continuum in Raman scattering at 100 cm⁻¹ corresponds roughly to two times the energy at which the continuum is observed in neutron scattering.¹⁶ However, the value of the gap-induced mode in Raman scattering at 30 cm⁻¹ $\approx 43\text{K}$ is markedly smaller than two times the singlet-triplet transition, $\Delta_g = (01\frac{1}{2}) = 24\text{--}30\text{K}$ derived from neutron scattering.^{15,16} This points to strong attractive magnon-magnon interaction in the Raman process.³¹ A second mechanism for a gap-induced mode may be a singlet bound state that splits off from the singlet-triplet excitation and is renormalized due to dimer-dimer interaction.⁵ Using RPA an estimate of $\sqrt{3}\Delta_g = (01\frac{1}{2}) \approx 41\text{--}52\text{K}$ was given as the energy for this state.⁵ However, the spectral weight of this bound state in Raman scattering is calculated to be negligible.³¹

In Figs. 2 and 3 the Raman spectra of $(\text{Cu}_{1-x}\text{Zn}_x)\text{GeO}_3$ and $\text{Cu}(\text{Ge}_{1-y}\text{Si}_y)\text{O}_3$ are presented for $x = 0, 0.018, 0.06$ and $y = 0.022, 0.06, 0.1$, respectively, at (a) 5 K and (b) 40 K. At first glance the spectra of $(\text{Cu}_{1-x}\text{Zn}_x)\text{GeO}_3$ look very similar. Indeed, no big changes of the dominant phonons were observed. However, the gap-induced mode in $(\text{Cu}_{1-x}\text{Zn}_x)\text{GeO}_3$ decreases strongly for $x = 0.018$ and disappears for all $x > 0.018$ [Fig. 2(a)]. For any Si substitution investigated as shown in the

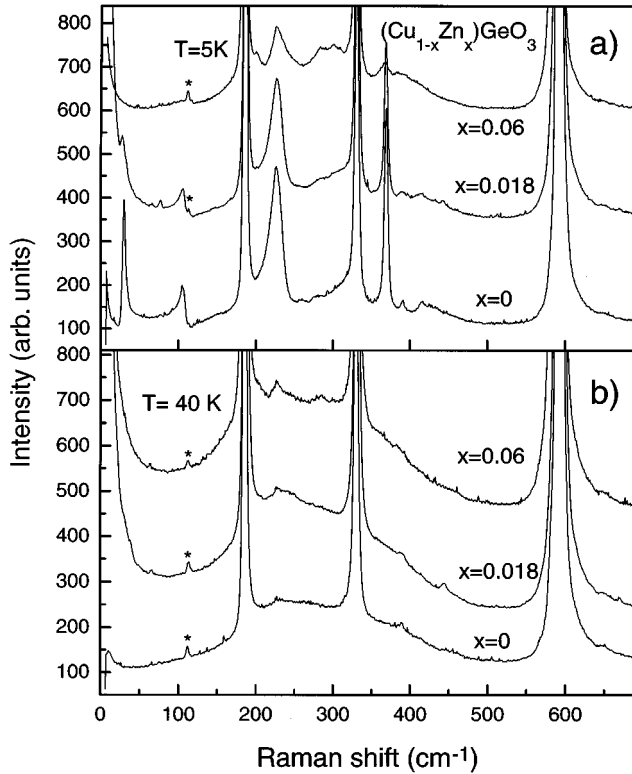


FIG. 2. Scattering intensity of $\text{Cu}_{1-x}\text{Zn}_x\text{GeO}_3$ with $x=0$, 0.018, 0.035, and 0.06 at (a) 5 and (b) 40 K. The curves are shifted by a subsequent addition of 200 a.u. Additional symmetry forbidden modes due to a slight misalignment of the sample are marked by an asterisk.

upper panel of Fig. 3 the gap-induced mode is not visible. The Peierls-induced phonon modes at 105 and 370 cm^{-1} and the peak of the two-magnon density of states for $T < T_{\text{SP}}$ are also reduced in intensity with increasing Zn and Si substitution. However, their appearance for higher x and y values extends now to temperatures well above T_{SP} . This is most clearly seen in Fig. 3(b) for the highest Si content $y=0.1$, but is also observed for smaller y or for Zn substitution with $x=0.06$. This effect will be analyzed below in Fig. 6. The spinon continuum observable above T_{SP} and with a reduced intensity in the pure system below T_{SP} is unchanged in magnitude in the case of Zn substitution up to $x=0.06$. With this value a maximum coherence length of the spinon excitations in the uniform state of 50 Å is calculated. Theoretical estimates¹³ lead to coherence lengths of the order of $\xi_0 \sim (J/\Delta_{\text{SP}})a = 15\text{--}20$ Å, with the lattice parameter $c = 2.94$ Å. Additionally, the decrease of the continuum intensity is prohibited for $x \geq 0.035$ due to a quenching of the spin-Peierls gap.

The overall intensity of the continuum is modified for Si substitution: We observe a gradual decrease of the continuum intensity with increasing y . The integrated intensity of the continuum for different x and y of both $(\text{Cu}_{1-x}, \text{Zn}_x)\text{GeO}_3$ and $\text{Cu}(\text{Ge}_{1-y}, \text{Si}_y)\text{O}_3$ is presented in Fig. 4 as function of temperature. To facilitate a comparison of samples with different substitutions we normalized the data to the phonon intensity at 593 cm^{-1} for Zn substitution or to the background in the frequency region 500–550 cm^{-1} for

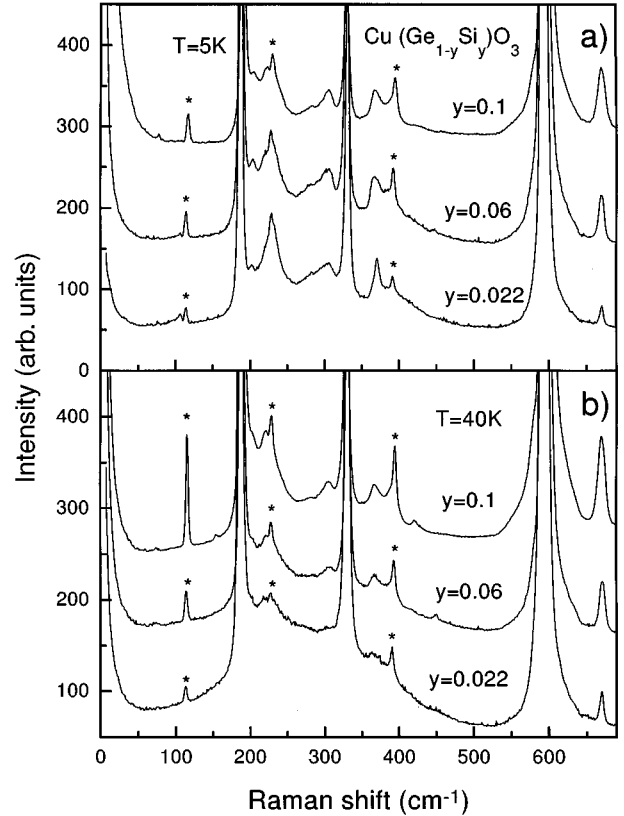


FIG. 3. Scattering intensity of $\text{Cu}(\text{Ge}_{1-y}, \text{Si}_y)\text{O}_3$ with $y=0$, 0.022, 0.06, 0.1 at (a) 5 and (b) 40 K. The curves are shifted by a subsequent addition of 100 a.u. Symmetry forbidden modes of the pure compound that are induced by Si substitution are marked by an asterisk. The phonon at 690 cm^{-1} is a defect mode.

the Si substituted samples. The background as reference for $\text{Cu}(\text{Ge}_{1-y}, \text{Si}_y)\text{O}_3$ was chosen because of the non-negligible dependency of the phonon intensity on Si substitution. In Fig. 4(a) the continuum intensity of $(\text{Cu}_{1-x}, \text{Zn}_x)\text{GeO}_3$ shows for $x=0$ and 0.018 still a decrease below T_{SP} of comparable size. For $x \geq 0.035$ this decrease is absent. In $\text{Cu}(\text{Ge}_{1-y}, \text{Si}_y)\text{O}_3$ the integrated intensity shows for $y=0.022$ and 0.06 a suppression of intensity below 40 K compared with $y=0$. This suppression results for $y=0.1$ in an overall smaller intensity of the continuum over the whole temperature region investigated (5–300 K). This effect on the frustration-induced scattering intensity is naturally attributed to a change of frustration ($\beta - \alpha$) in H_R and H for the case of Si substitution. As β involves mainly excited orbital superexchange that may not be changed by substitution the reduced scattering intensity of the continuum is attributed to an enlarged α . This is supported by the strong sensitivity of α on pressure and the large variation of the lattice parameters observed with Si substitution.²⁷ Raman experiments with applied pressure were used to estimate an increase of α of 30% for a pressure of 5 GPa.³² The lattice pressure observed in Si substitution should lead to a similar effect and increase α . As in Zn-substituted samples, no large change of the lattice parameters exists²⁵ we also do not observe an overall smaller intensity of the continuum for this substitution. It should be noted that the local character of the Raman exchange process may be especially sensitive to local changes of the exchange path that are not visible in thermo-

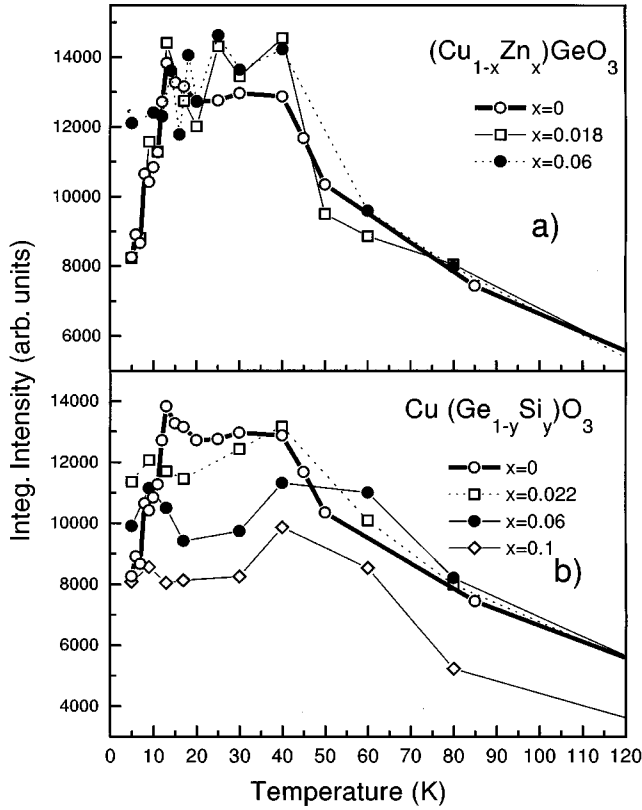


FIG. 4. Integrated intensity of the spinon continuum between 100 and 500 cm^{-1} for (a) $\text{Cu}_{1-x}\text{Zn}_x\text{GeO}_3$ with $x=0, 0.018, 0.06$ and (b) $\text{Cu}(\text{Ge}_{1-y}\text{Si}_y)\text{O}_3$ with $y=0, 0.022, 0.06, 0.1$ in dependence of temperature. A linear background, phonons, and additional modes were subtracted from the data prior to integration. The data on $\text{Cu}_{1-x}\text{Zn}_x\text{GeO}_3$ were normalized to the phonon at 593 cm^{-1} while the data on $\text{Cu}(\text{Ge}_{1-y}\text{Si}_y)\text{O}_3$ were normalized on the background between 500 and 550 cm^{-1} to facilitate the comparison between different x, y , respectively.

dynamic types of experiments. Indeed no shift of the broad maximum in the magnetic susceptibility was found in Si-substituted samples.²⁷ Therefore we propose neutron scattering as a key experiment to verify this result.

The gap-induced mode is replaced at low temperatures (5 K) by a gradual increase of intensity for $\omega \rightarrow 0$, both visible for Si and Zn substitution (see Fig. 5). The quasielastic scattering of diffusive origin shows a continuous overall decrease of intensity with decreasing temperature 60 to 30 K. Below 15 K, however, the intensity of the quasielastic scattering increases again. This peculiar temperature dependence points to a nontrivial origin of the low temperature signal,^{33–35} i.e., not to scattering on static lattice defects but to very low energy excitations of the spin system as they are predicted for doped spinons in substituted spin chains.³³ It is remarkable that this intensity decreases again in the Néel state of $(\text{Cu,Zn})\text{GeO}_3$ at, e.g., $T=1.8$ K in Fig. 5(a).

In- and off-chain substitutions lead to anomalies in the Raman intensity that will be discussed here in the framework of a dimensional crossover of CuGeO_3 . Both, the two-magnon cutoff peaking at 226 cm^{-1} and the phonon mode at 370 cm^{-1} are observed in substituted samples above the transition temperature of the pure compound. In Fig. 6 the normalized, integrated intensity of the 370 cm^{-1} phonon is

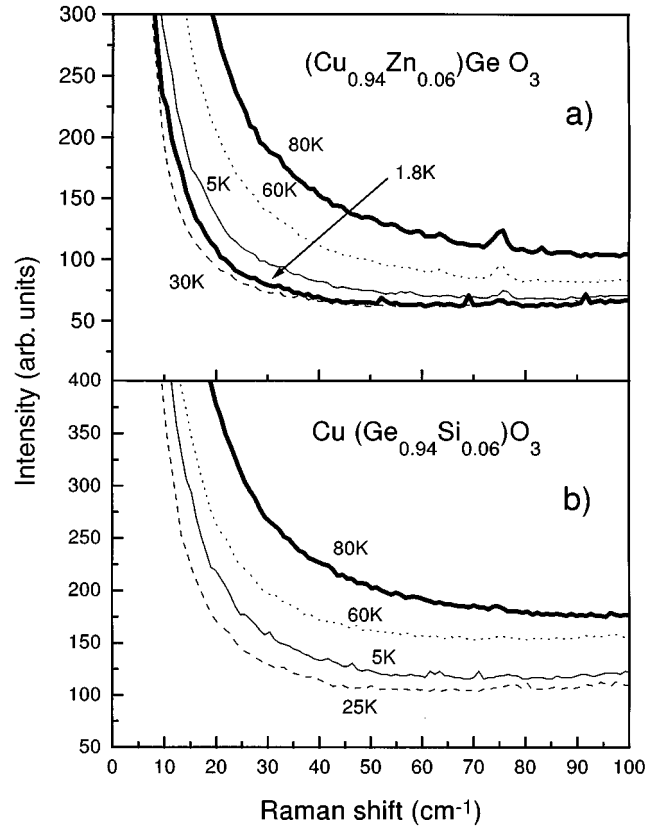


FIG. 5. Quasielastic scattering in (a) $\text{Cu}_{0.94}\text{Zn}_{0.06}\text{GeO}_3$ and (b) $\text{Cu}(\text{Ge}_{0.94}\text{Si}_{0.06})\text{O}_3$ for different temperatures. The signal at $T=30$ and 25 K remains from straylight. The intensity at $T=5$ K is above this level.

shown for different Si and Zn substitutions. For the pure compound the onset of this mode is visible as a shoulder starting at T_{SP} and increasing sharply below 12 K [see for comparison Fig. 1(b) on an enlarged scale]. It reaches half its maximum intensity at $T_{\text{cross}}=11$ K. For Si-substituted samples T_{cross} is determined to be 25 K ($y=0.02$), 35 K ($y=0.06$), and 50 K ($y=0.1$). For Zn-substitution this mode is visible for $x=0.06$ at $T_{\text{cross}}=23$ K with 10% intensity of the pure sample. With lower Zn-substitution levels the intensity is less reduced. However, the shift of the crossover temperature above T_{cross} of the pure compound is not as obvious as in the case of Si substitution. In Table I, a comparison of the characteristic temperatures of all substituted samples is given. The shift of T_{cross} above T_{SP} takes place for in-chain substitution with $x \geq 0.035$ while for off-chain substitution only $y \geq 0.005$ is needed. This later value is determined by a linear extrapolation of the characteristic temperatures in dependence on y . The crossover is independent of the Néel temperature.

IV. DISCUSSION

To understand the properties of CuGeO_3 , the coupling of spin degrees of freedom to the lattice and the interchain interaction should be considered. This interplay is demonstrated in the behavior and dimensionality of the low-energy excitations observed in Raman scattering. Indeed, the two-magnon density of states below 226 cm^{-1} resembles 3D

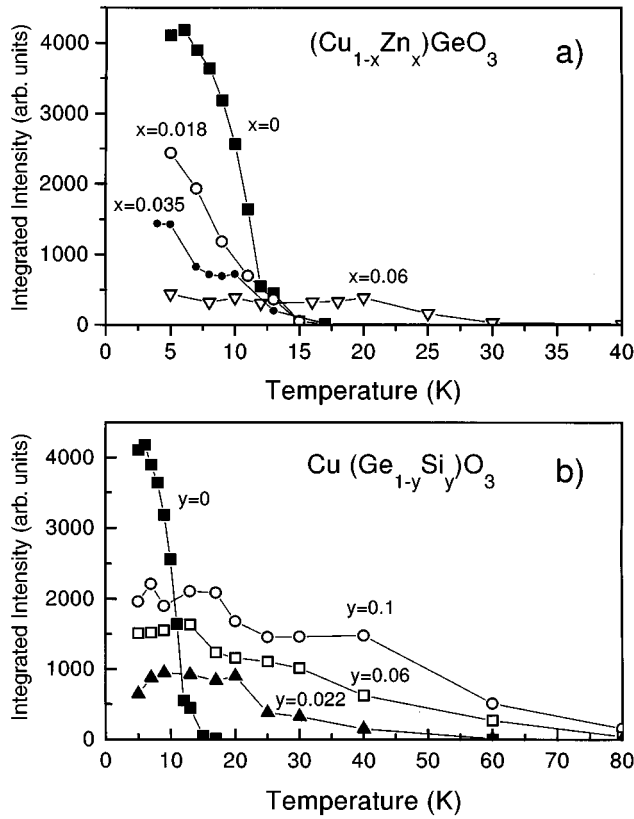


FIG. 6. Normalized integrated intensity of the spin-Peierls-induced phonon mode at 370 cm^{-1} for $\text{Cu}_{1-x}\text{Zn}_x\text{GeO}_3$ and $\text{Cu}(\text{Ge}_{1-y}\text{Si}_y)\text{O}_3$. T_{cross} is defined from these data as the temperature of half maximum intensity of the phonon.

excitations as it is fairly well described in a spin-wave approximation of a 3D Heisenberg system.^{21,22} The additional phonon modes at 105 , 370 , and 820 cm^{-1} undoubtedly have 3D character. The gap-induced mode at 30 cm^{-1} and the spinon continuum, however, are attributed to 1D spinon excitations.²³ Hints towards excitations of mixed character exist in terms of a Fano line shape of the spin-Peierls-induced phonon at 105 cm^{-1} and a high energy shoulder of the continuum above 400 cm^{-1} that is not suppressed below T_{SP} [see Fig. 1(a)]. The low-energy maximum of this tail at 414 cm^{-1} corresponds to the sum of the phonon at 370 cm^{-1} and the spin-Peierls gap at the zone center, $\Delta_q = (\frac{1}{2}0\frac{1}{2}) = 44 \text{ cm}^{-1}$.²⁰

The intensity of the Peierls-active phonon at 370 cm^{-1} and the two-magnon peak scale with each other in their dependence on temperature and, on the other hand, compete with the spinon continuum intensity. As the key observation in our study, this leads to the following conclusions: The interchain interaction itself is important, but not sufficient to explain this rapid crossover in intensities. It should only lead to gradual changes of the spin dynamics below a 3D coherence temperature $T_{3\text{D}} = k_B J_b \approx 15 \text{ K}$. However, the rotational invariant order of spin dimers formed at the spin-Peierls transition triggers this crossover due to a rapid change of the $s = 1/2$ spinons to propagative $s = 1$ excitations.⁵ Both interchain and long range magnetoelastic interactions increase the k phase space of the magnons from 1D to 3D and fix a long

range ordered arrangement of dimers on the chains. This may result in a “confinement” of the spin degrees of freedom and a decreasing spin-spin correlation length with increasing temperature. A correct model should therefore include a coherence length of 3D correlated spin dimers that is obviously temperature dependent. Until now no such theory exists. Therefore we use arguments derived on substituted spin ladders.

Recently, the theoretical study of nonmagnetic impurities in spin chains and ladders gained interest as a first step towards understanding correlation effects in doped quantum spin systems.^{33,36–39} In earlier Monte Carlo studies of the spin susceptibility in random or disordered, nondimerized spin chains a suppression of the long range AF correlations and an enhancement of the spin-Peierls instability was found.^{34,35} Recent theoretical investigations of strongly dimerized spin chains show that nonmagnetic impurities create loose $s = 1/2$ spins which randomly introduce states within the magnetic excitation gap. These states should be observable as low energy excitations (doped spinons) that form a weakly dispersing impurity branch inside the gap. For realistic, smaller values of dimerization an effective spin $s = 1/2$ is spread over several lattice spacings leading to many-body $s = 1/2$ states. These states enhance the spin-spin correlation at short distances.^{33,37} In close relation to these effects, studies of spin ladders propose a quantum phase transition from a gapped state to a quantum critical state even at low impurity concentrations ($\approx 1\%$).³⁷ Above this concentration a bulk spin state with no excitation gap and a long range, algebraic decay of the spin-spin correlations are predicted for Zn-doped spin ladders.³⁷ The above-mentioned effects were discussed in the substituted spin ladder $\text{Sr}(\text{Cu},\text{Zn})_2\text{O}_3$.^{33,40}

The conclusion drawn from Raman experiments critically depends on the interpretation of the two-magnon signal and the quasimagnon dispersion seen in neutron scattering. It was demonstrated using neutron scattering on CuGeO_3 (Ref. 16) that excitations with small k , close to $k_{\text{AF}} = (0,1,0.5)$, are dominantly influenced by the dimerization while the character of the magnons in the middle of the Brillouin zone still resembles those of the spinons in the uniform chain. Therefore excitations at low energy close to Δ_{SP} should respond most strongly to an increase of temperature or impurity content in the compound. Actually we see a strong broadening and a shift of the gap-induced mode close to T_{SP} and its vanishing in substituted samples while the two-magnon signal is only influenced in intensity.

In substituted samples we still see a similar behavior of the phonon and two-magnon intensities as shown in Figs. 2 and 3. However the temperature range is shifted upwards. The general existence of this scattering intensity and the shift of T_{cross} above T_{SP} of the pure compound may only be understood if an increased short range tendency towards dimerization exists at higher temperature. This is seen in Monte Carlo studies on disordered spin chains as an enhanced four-spin susceptibility.³⁴ Similar results on substituted spin ladders point to an increased spin-spin correlation near an impurity.^{33,37} In our case this enhanced correlation leads to a localization of a spin dimer at the impurity site. The crossover that was triggered by the opening of the gap in the pure compound is therefore now observed at higher temperatures with T_{cross} proportional to the impurity content. Si substitution introduces more disorder compared with the local dis-

ruption of the spin chains using Zn substitution. Therefore the increase of T_{cross} is more pronounced in this case. Our observations of a preferred spin-Peierls instability against competing AF correlations in disordered spin chains are in good agreement with theory.³⁴

As shown in the previous sections, the spin-Peierls active modes react in various ways on substitution. This difference is in part originated in the different coherence length of the excitations involved. The 1D spinon continuum is observed both in pure and substituted samples. By the opening of the spin-Peierls gap this intensity is reduced due to the localizing, pair-binding effect of the excitation gap. No drop in the continuum intensity is observed for sufficiently large Zn ($x > 0.03$) or Si substitution ($y > 0.02$). The survival of the continuum, independent of substitution, clearly stresses the short range character of these excitations in the dimerized phase.

In general it is quite striking that only a small amount of substitution is required to completely suppress the spin-Peierls transition, independent of the substitution site. The important point seems to be that the system is disturbed by substitution. The appearance of Néel ordering in a limited concentration range starting above $\approx 1\%$ for both substituted CuGeO_3 and the spin ladder system SrCu_2O_3 points to a similar instability. A proposed quantum phase transition^{33,37} in weakly substituted spin ladders is a promising concept to describe this behavior as it also gives hints towards the disappearance of T_N at higher concentrations. Here the long ranged resonating valence bond state gets energetically unfavorable again. To interpret the appearance and consequent disappearance of T_N simply due to interchain coupling and a following frustration of the 3D ordered spin system would not be appropriate as the pure compound is already strongly frustrated. The absence of any additional magnetic scattering for $T \leq T_N$ in CuGeO_3 is quite striking. This means that on the local scale of exchange scattering no additional scattering channel opens up going from the regime of short range AF fluctuations with coexisting local singlet formation to the truly ordered 3D AF state. However, the quasielastic scattering observed at low temperatures in substituted samples attributed to low lying defect-induced spin excitations disappears in the Néel state.

V. CONCLUSIONS

Using Raman scattering the effect of in-chain and off-chain substitutions on spin fluctuations and spin-Peierls active modes was investigated. The observed scattering modes respond differently on changes of the temperature and on substitutions. The gap-induced mode showing up below T_{SP} strongly decreases in intensity upon Zn and Si substitution. Additionally, the drastic decrease of the integrated spinon continuum below T_{SP} is suppressed in substituted samples due to a quench of the spin-Peierls gap. This effect does not depend on the kind of defect and is in agreement with magnetic susceptibility measurements on substituted CuGeO_3 .²⁶ However, the decrease of the spinon continuum that was observed above T_{SP} only for Si substitution is tentatively attributed to lattice pressure-induced changes of the frustration. Si substitution leads to the largest changes of the lattice parameters of all investigated substitutions.²⁵

The modes of 3D origin, i.e., the spin-Peierls induced phonon at 370 cm^{-1} and the two-magnon cutoff at 226 cm^{-1} compete in the pure samples with the 1D spinon continuum. A crossover temperature is proposed that marks a transition from 1D to 3D behavior of the coupled spin chains. This crossover is triggered by a 3D coherent singlet state with propagative magnon excitations arising due to the interchain interaction. In the substitution studies presented here the crossover temperature is shifted to higher temperatures due to enhanced spin-spin correlation at the impurity site. Additional antiferromagnetic low lying spin excitations are induced by the substitution. These observations are in good agreement with recent theoretical calculations of the spin response and behavior of the spin-spin correlation length in substituted spin ladders. This supports our idea of a general similarity between defect states in weakly coupled spin chains close to a spin-Peierls transition and spin ladders where the dimer formation is favored by topology.

ACKNOWLEDGMENTS

This work was supported by DFG, through SFB 341, SFB 252, and by BMBF 13N6586/8. We thank V. N. Muthukumar, W. Brenig, and P. H. M van Loosdrecht for extensive and helpful discussions.

¹G. Müller, H. Thomas, H. Beck, and J.C. Bonner, Phys. Rev. B **24**, 1429 (1981).

²J. des Cloizeaux and J.J. Pearson, Phys. Rev. **128**, 2131 (1962).

³D.A. Tennant, R.A. Cowley, S.E. Nagler, and A.M. Tsvetlik, Phys. Rev. B **52**, 13 368 (1995).

⁴M. Arai, M. Fujita, M. Motokawa, J. Akimitsu, and S.M. Benington, Phys. Rev. Lett. **77**, 3649 (1996).

⁵G.S. Uhrig and H.J. Schulz, Phys. Rev. B **54**, R9624 (1996); A. Fledderjohann and C. Gros, Europhys. Lett. **37**, 189 (1997).

⁶M. Hase, I. Terasaki, and K. Uchinokura, Phys. Rev. Lett. **70**, 3651 (1993).

⁷M. Nishi, O. Fujita, and J. Akimitsu, Phys. Rev. B **50**, 6508 (1994).

⁸H. Kuroe *et al.*, Phys. Rev. B **50**, 16 468 (1994).

⁹J.P. Boucher, L.P. Regnault, J. Phys. (France) I **6**, 1939 (1996).

¹⁰G. Castilla, S. Chakravarty, and V.J. Emery, Phys. Rev. Lett. **75**, 1823 (1995).

¹¹B. Büchner, U. Ammerahl, T. Lorenz, W. Brenig, G. Dhalenne, and A. Revcolevschi, Phys. Rev. Lett. **77**, 1624 (1996).

¹²M. Braden, G. Wilkendorf, J. Lorenzana, M. Ain, G.J. McIntyre, M. Behruzi, G. Heger, G. Dhalenne, and A. Revcolevschi, Phys. Rev. B **54**, 1105 (1996).

¹³D. Khomskii, W. Geertsma, and M. Mostovoy, Czech. J. Phys. **46**, 32 (1996).

¹⁴R. Chitra *et al.*, Phys. Rev. B **52**, 6581 (1995).

¹⁵M. C. Martin, G. Shirane, Y. Fujii, M. Nishi, O. Fujita, J. Akimitsu, M. Hase, and K. Uchinokura, Phys. Rev. B **53**, R14 713 (1996).

¹⁶M. Ain, J.E. Lorenzo, L.P. Regnault, G. Dhalenne, A. Revcolevs-

- chi, B. Hennion, and Th. Jolicoeur, Phys. Rev. Lett. **78**, 1560 (1997).
- ¹⁷L.P. Regnault, J.P. Renard, G. Dhalenne, and A. Revcolevschi, Europhys. Lett. **32**, 579 (1995).
- ¹⁸M. Hase, K. Uchinokura, R.J. Birgeneau, K. Hirota, and G. Shirane, J. Phys. Soc. Jpn. **65**, 1392 (1996).
- ¹⁹H. Fukuyama, T. Hamitomo, and M. Saito, J. Phys. Soc. Jpn. **65**, 1182 (1996).
- ²⁰P.H.M. van Loosdrecht *et al.*, Phys. Rev. Lett. **76**, 311 (1996); P.H.M. van Loosdrecht, J.P. Boucher, S. Huant, G. Martinez, G. Dhalenne, and A. Revcolevschi, Physica B (to be published).
- ²¹I. Loa, S. Gronemeyer, and C. Thomsen, Solid State Commun., **99**, 4, 231–235 (1996).
- ²²P. Lemmens, B. Eisener, M. Brinkmann, L.V. Gasparov, G. Güntherodt, P.v. Dongen, M. Weiden, W. Richter, C. Geibel, and F. Steglich, Physica B **223&224**, 535 (1996); P. Lemmens, M. Udagawa, M. Fischer, G. Güntheroth, M. Weiden, W. Richter, C. Geibel, and F. Steglich, Czech. J. Phys. **46**, 1979 (1996); M. Fischer, P. Lemmens, G. Güntherodt, M. Weiden, W. Richter, C. Geibel, and F. Steglich, Physica B (to be published).
- ²³V.N. Muthukumar, C. Gros, W. Wenzel, R. Valentí, P. Lemmens, B. Eisener, G. Güntherodt, M. Weiden, C. Geibel, and F. Steglich, Phys. Rev. B **54**, R9635 (1996); V.N. Muthukumar, C. Gros, R. Valentí, M. Weiden, C. Geibel, F. Steglich, P. Lemmens, M. Fischer, and G. Güntherodt, Phys. Rev. B **55**, 5944 (1997).
- ²⁴P.A. Fleury and R. Loudon, Phys. Rev. **166**, 514 (1967).
- ²⁵M. Weiden, W. Richter, C. Geibel, F. Steglich, P. Lemmens, B. Eisener, M. Brinkmann, and G. Güntherodt, Physica B **225**, 177 (1996).
- ²⁶M. Weiden, W. Richter, R. Hauptmann, C. Geibel, and F. Steglich, Physica B (to be published).
- ²⁷M. Weiden, R. Hauptmann, W. Richter, C. Geibel, P. Hellmann, M. Köppen, F. Steglich, M. Fischer, P. Lemmens, G. Güntherodt, A. Krimmel, and G. Nieva, preceding paper, Phys. Rev. B **55**, 15 067 (1997).
- ²⁸J.P. Renard, K. deDang, P. Veillet, G. Dhalenne, A. Revcolevschi, and L.P. Regnault, Europhys. Lett. **30**, 475 (1995).
- ²⁹M. Fischer, P. Lemmens, G. Güntherodt, M. Weiden, C. Geibel, and F. Steglich (unpublished).
- ³⁰M.G. Cottam, and D.J. Lockwood, *Light Scattering in Magnetic Solids* (Wiley-Interscience, New York, 1986).
- ³¹C. Gros, W. Wenzel, A. Fledderjohann, P. Lemmens, M. Fischer, G. Güntherodt, M. Weiden, C. Geibel, and F. Steglich, this issue, Phys. Rev. B **55**, 15 048 (1997).
- ³²P.H.M. van Loosdrecht, J. Zeman, G. Martinez, G. Dhalenne, and A. Revcolevschi, Phys. Rev. Lett. **78**, 487 (1997).
- ³³G.B. Martins, E. Dagotto, and J. Riera Phys. Rev. B **54**, 16 032 (1996).
- ³⁴J.E. Hirsch and R. Kariotis, Phys. Rev. B **32**, 7320 (1985).
- ³⁵H.-B. Schüttler, D.J. Scalapino, and P.M. Grant, Phys. Rev. B **35**, 3461 (1987).
- ³⁶H. Fukuyama, N. Nagaosa, M. Saito, and T. Tanimoto, J. Phys. Soc. Jpn. **65**, 2377 (1996).
- ³⁷Y. Motome, N. Katoh, N. Furukawa, and M. Imada, J. Phys. Soc. Jpn. **65**, 1949 (1996).
- ³⁸N. Nagaosa, A. Furusaki, M. Siegrist, and H. Fukuyama, J. Phys. Soc. Jpn. (to be published).
- ³⁹Y. Iino and M. Imada (unpublished).
- ⁴⁰M. Azuma, Y. Fujishiro, M. Takano, T. Ishida, K. Okuda, M. Nohara, and T. Takagi (unpublished).